CHAPTER III

EXISTENCE OF MICRODOMAIN ORIENTATION IN THERMOPLASTIC ELASTOMER THROUGH A CASE STUDY OF SEBS ELECTROSPUN FIBERS

3.1 Abstract

Although the microdomains of polymeric systems including the thermoplastic elastomers in the as-spun electrospun fiber were reported, the orientation of microdomains has not yet been well clarified. The present work shows an existence of microdomain orientation through a case study of a well-aligned electrospun fibers of polystyrene-block-poly(ethylene-co-1-butene)-block-polystyrene triblock copolymer (SEBS) obtained from an electrospinning unit equipped with a rotational disk fiber-collector. Two-dimensional small-angle X-ray scattering (2D-SAXS) patterns of the as-spun electrospining SEBS fibers show elliptical and four-point patterns suggesting an orientation of distorted and fragmented lamellar microdomains. The electrospun fibers obtained from a low rotational disk collector speed (31.5 m/min) exhibits a significant microdomain distortion whereas the fibers obtained from high take-up velocities (310 m/min, 620 m/min, and 1240 m/min) show higher fragmented-microdomain stretching. By annealing the electrospun fibers, the fibers develop an isotropic SAXS pattern with traces of the remained anisotropic orientation. Based on the above mentioned evidences in SEBS, the present work, for the first time, clarifies that the as-spun thermoplastic elastomers fibers show not just a simple microdomain as used to be observed by transmission electron microscope (TEM) but rather with orientation which can be confirmed by SAXS.

Keywords: SEBS; Electrospun Fiber; Microdomains; Thermoplastic Elastomer; Microdomain Orientation

3.2 Introduction

For decades, the uses of thermoplastic elastomers (TPEs) have been increasing due to advantages of thermoplastic and elastomeric properties related to high strength and toughness. At present, the development of TPEs has reached a certain level where a variety of TPE copolymers are available.[1,2] Polystyrene-b-poly(ethylene-co-1-butene)-b-polystyrene triblock copolymer (SEBS) is one of the earliest developed TPEs and is used in daily-use tools, automotive parts, construction adhesives, and so on, because of their superior weathering resistance resulting from the hydrogenation of unsaturated chemical linkages.[3-5] The SEBS consists of a hard block (polystyrene block, or S block) and a soft block (poly(ethylene-co-butene) block, or EB block). This material is a typical block copolymer with self-aggregation of the internal structure. Since the solubility parameters of these two blocks are significantly different, microphase separation of the S microdomains in the EB matrix is generated, especially when the styrene content is less than 30 %.

Up to present, various microphase-separated morphologies of polystyrene based block , mostly in films, have been reported , for example, spherical,[6] cylindrical,[7,8] and lamellar shape.[9] The morphology of microdomains are found to be depending on several factors, such as polystyrene weight fraction,[10] solvent type,[11,12] and temperature,[13,14] etc. Several examples of TPEs in film form have been reported about microdomain distortion and its orientation including how microdomain induced specific mechanical properties.[15,16]

Electrospinning is known as a technique for fabricating ultrafine fiber, ranging from nano- to micro-scale via electric force.[17] In the case of TPEs, electrospinning might be an effective way to utilize an intense stress in a confined geometry to control the microdomain orientation as seen in thermoplastic case. For example, Fong and Reneker reported a small and peculiar shape of phase-separated domain in the electrospun fibers of a polystyrene-b-polybutadiene-b-polystyrene triblock copolymer (SBS) due to high evaporation rate of volatile solvents and at that time the polymer chain mobility was limited to end up with a segregation in a thermodynamically equilibrated microdomain structure.[18] Ma et al.[19] and Kalra et al.,[20] showed the relevant results, especially a small and disordered structure of the

microdomains, which were termed as the non-equilibrium state of microphase separation in electrospun TPEs, as evidenced from transmission electron microscope (TEM) images.

Up to present the lamellar microdomains and their orientation of the TPE films have been reported and it seems that the microdomains of the films are similar to those of the fibers. In the case of SEBS film, it was reported that the microdomain orientation of SEBS was due to shear force.[21] For fibers, although electrospinning is a technique that favors the chain alignment to give orientation of the microdomain morphology, to our best knowledge there is no report related to microdomain orientation in the as-spun fiber. Most dealt with the electrospun fibers with irregular microdomain which an annealing and stretching process further develops fiber orientation.

Surprisingly, when we prepared the SEBS fibers by using an electrospinning system equipped with a rotational disk collector which can control the speed of the fiber collector followed by a careful morphology analysis based on SAXS patterns, we found anisotropic microdomain orientation existed in our SEBS. In other words, the results confirm that there is microdomain orientation in the TPEs fibers. The present work, thus, aims to show an existence of microdomain orientation in TPEs through a case study of electrospun SEBS which the factors involved in microdomain orientation in the fibers such as the control of fiber alignment via an electrospun system equipped with disk collector and the annealing process were also taken in our consideration.

3.3 Experimental

3.3.1 Materials

SEBS triblock copolymer (specification: 32 wt % styrene content, Mw = 80 000 g/mol and Mn =50 000 g/mol, and melt flow index = 5 g/10mins (230°C for 2.16 Kg)) was a gift from Asahi Kasei Chemicals Cooperation, Japan. Chloroform and toluene were purchased from Nacalai Tesque, Inc., Japan. All chemicals were used without further purification.

SEBS solutions (18 % w/w) were prepared by dissolving SEBS in chloroform/toluene (80/20 wt/wt) mixed solvent. The homogeneous solution was cast on the teflon sheet, and dry it at room temperature for 7 days.

3.3.3 Preparation of SEBS electrospun fibers

SEBS solution (18 % w/w) was prepared by dissolving SEBS in chloroform/toluene (80/20 wt/wt) mixed solvent. The homogeneous solution obtained was electrospun to fibers by using a Nanon Electrospinning Setup (MECC Co., Ltd., Japan) equipped with an originally designed rotational disk collector. The spinning conditions were: accelerated voltage, 20 kV; volumetric flow rate, 0.5 mL/h; and tip-to-collector distance, 15 cm. The fibers were collected onto an aluminium foil. The take-up velocity of the rotational disk collector was varied, i.e., 31.5 m/min, 310 m/min, 620 m/min and 1 240 m/min. The relative humidity for spinning was in the range of 30-32 %.

3.3.4 Characterizations

The surface of the SEBS electrospun fiber was observed by a JEOL JSM-5200 scanning electron microscope, and the average fiber diameter was determined by Image J software. The fiber-alignment appearances were observed by a Hitachi-TM3000 Tabletop Microscope (TM) with accelerating voltage of 5kV. TEM observation, the fibers were stained with ruthenium tetroxide vapor (RuO_4) and microtomed at room temperature before taking the images by a Hitachi TEM Zero H-7650 with accelerating voltage of 100 kV. The two-dimensional small-angle X-ray scattering (2D-SAXS) measurements were carried out at the RIKEN structural biology beamline I (BL45XU) SPring-8, Hyogo, Japan. The 2D-SAXS patterns (300 mm x 300 mm area) were recorded using a RIGAKU R-AXIS IV++ equipped with an imaging plate detector. The X-ray wavelength, λ, was tuned at λ= 0.10 nm, and the q values defined by $q = (4\pi/\lambda) \sin(\theta/2)$ (θ : scattering angle) were calibrated by chicken tendon collagen having the spacing of 65.3nm.

3.4 Results and Discussion

In order to control the microdomain structures in the SEBS fibers, the fibers were prepared under a variation of fiber stretching force based on the adjustable take-up velocity (from 31.5 m/min to 1 240 m/min). To simplify our work, the electrospinning parameters were preliminary studied to select the optimal conditions. The optimal fiber spinning condition was; SEBS solution (80:20/chloroform: toluene) 18 % w/w under an accelerated spinning voltage of 20 kV. The above mentioned condition gives beadless fibers with a 6.0 μm diameter (Figure 3.1(a)). However, the fibers contain some pores with diameters of 150-240 nm (Figure 3.1(b)) which could be eliminated after the relative humidity was adjusted to be 23 % (Figure 3.1(c), 3.1(d)).

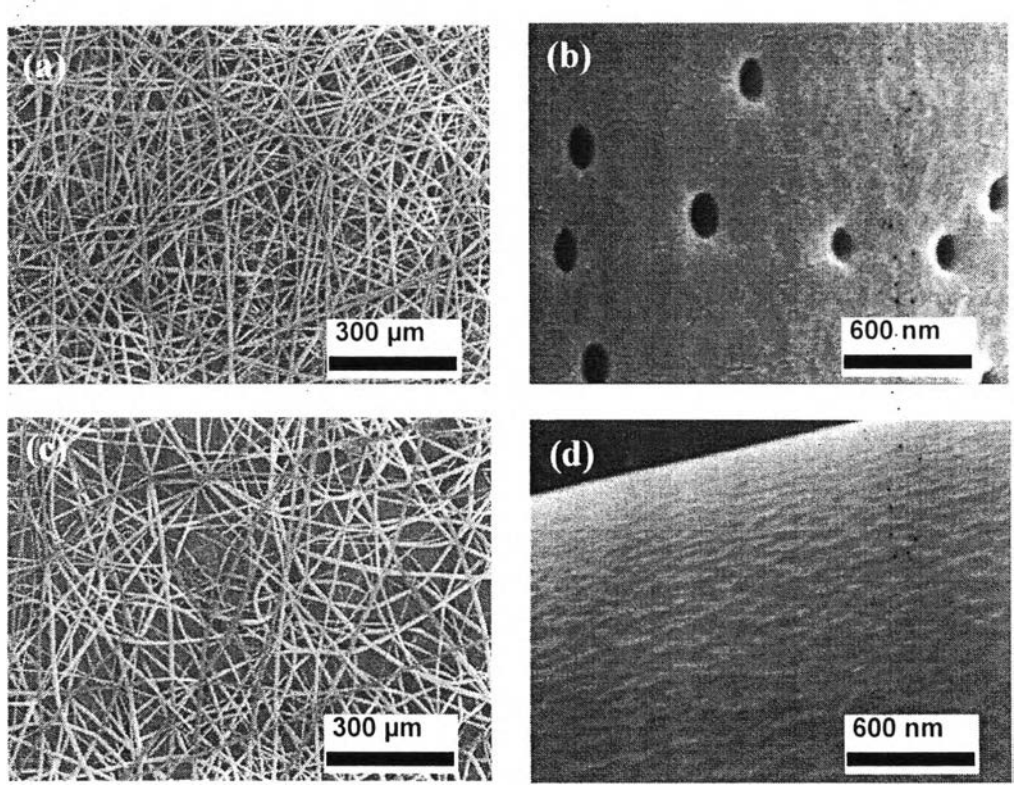

Figure 3.1 SEM micrographs of SEBS electrospun microfibers obtained from an accelerating voltage of 20 kV: (a) and (b) under 30 % RH; (c) and (d) under 23 % RH.

3.4.1 Microdomain Morphology

Fong and Reneker reported confined microdomains in electrospun nano-fiber. The report also showed an irregular shape of the microdomains under an elongational flow.[18] Kalra et al. pointed out that the irregular microdomains were inevitable as it was generated via a non-equilibrium state of fiber spinning. This point is different from the case of film where regular microdomains obtained from an equilibrium state.[20] Ma et al. demonstrated a long-range order of lamellar and spherical microdomain structures for triblock and diblock copolymers, respectively, by using a two-fluid coaxial electrospinning technique to maintain the shape of fiber during annealing.[19] Here, an attempt to identify the microdomains in the fibers was made by using a cross-sectional microtoming TEM. As shown in Figure 3.2(a)-(b), small and irregular microdomains are observed which appear to be similar to those in previous reports.[18-20]

The microdomain structure was further investigated by using 2D-SAXS technique. In this step, the fibers were carefully aligned during the fibers deposited on the disk collector and the alignment was confirmed by TM micrographs (Figure 3.3 (a)) before carrying out 2D-SAXS measurement. It should be noted that the fibers alignment appearances obtained from the high take-up velocity (Figure 3.3 (a)) and the low one (Figure 3.3 (b)) are similar. Figure 3.3(c) shows a 2D-SAXS pattern of SEBS with intense streaks ascribed to the total reflection of X-ray from the surface of fibers. Figure 3.3(e) shows a sample chamber attachment in which a particular solvent was filled. As the electron density of ethanol is close to that of the SEBS fibers, the total reflection was almost eliminated. Figure 3.3(d) shows a 2D-SAXS pattern after applying the contrast-matching method using an ethanol chamber (see more discussion in Figure 3.4B(a)). This means that by using this ethanol chamber, we can observe microdomains in details without the disturbance of streaks.

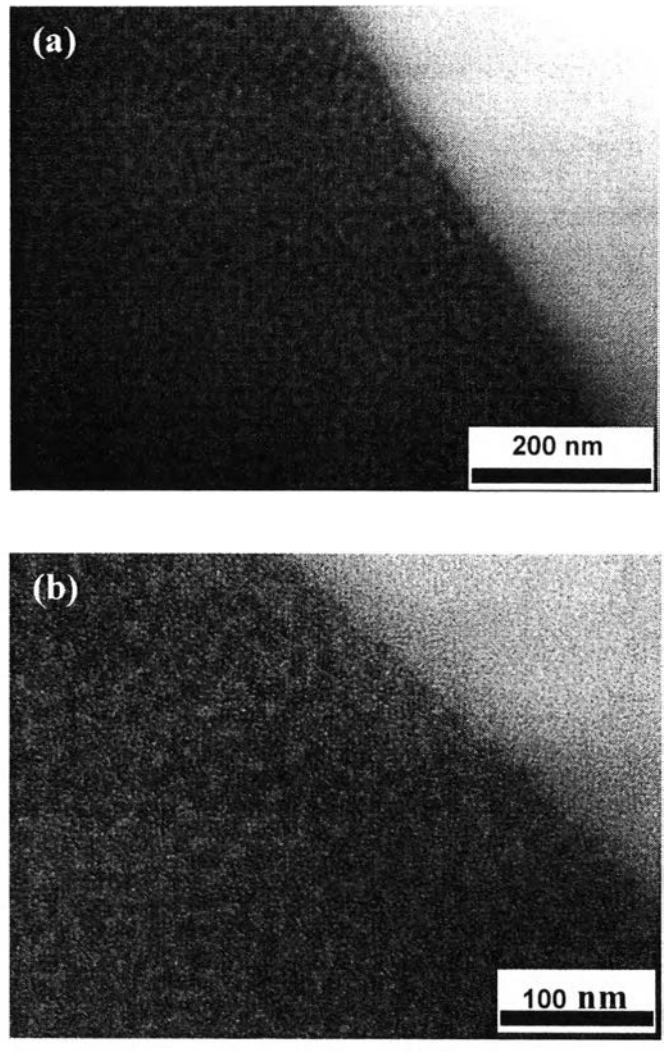

Figure 3.2 Cross-sectional TEM micrograph of SEBS electrospun fibers collected at a 1240 m/min take-up velocity at: (a) 25000 times and (b) 40000 times for magnification. PS microdomains stained with ruthenium tetroxide were appearing dark.

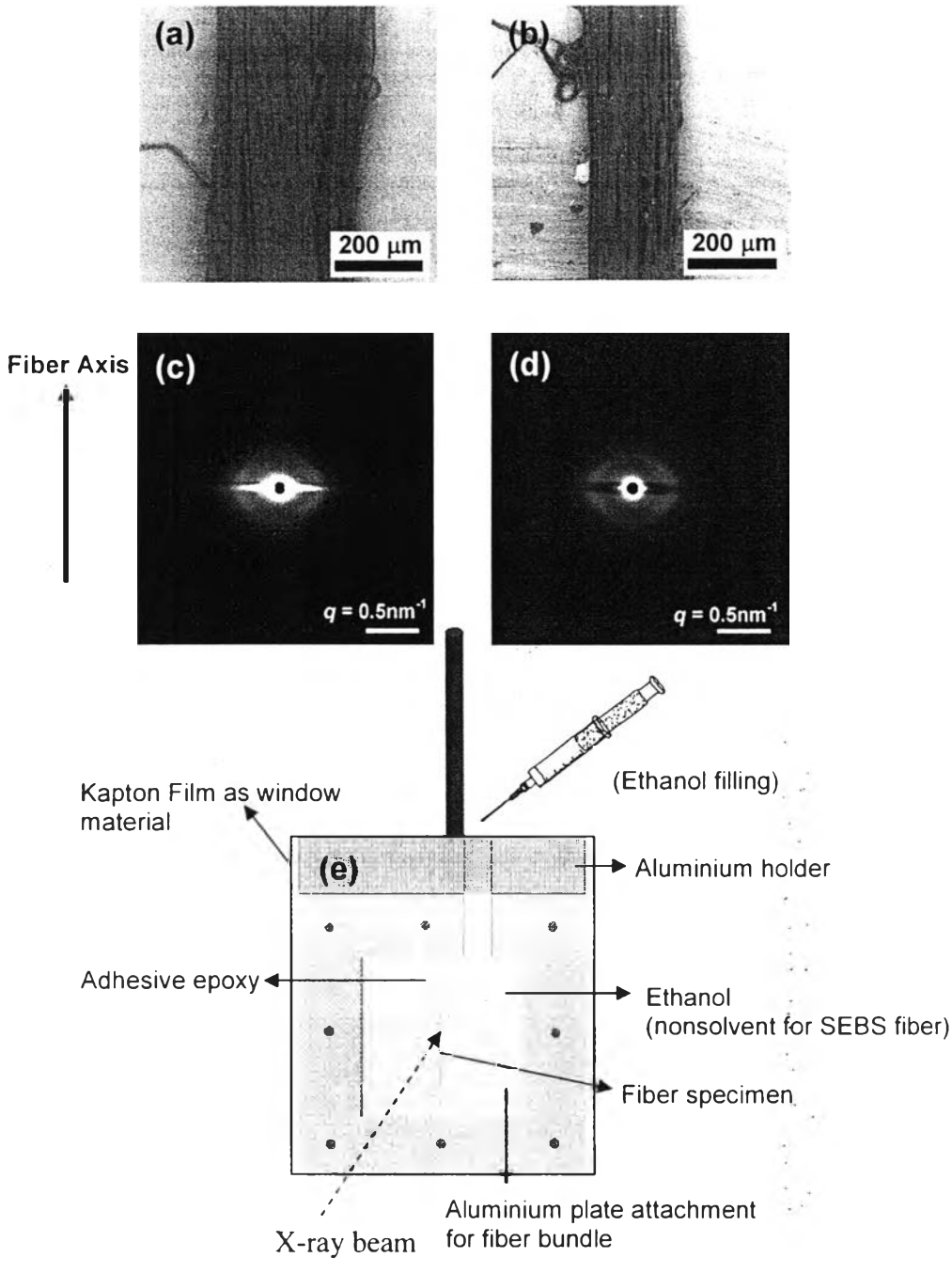

Figure 3.3 TEM micrographs of SEBS electrospun fibers collected at (a) 31.5 m/min, and (b) 1 240 m/min; and 2D-SAXS patterns of SEBS electrospun fibers collected at 31.5 m/min for: (c) in an air chamber, and (d) in ethanol-filled chamber; and (e) illustration of ethanol-filled chamber.

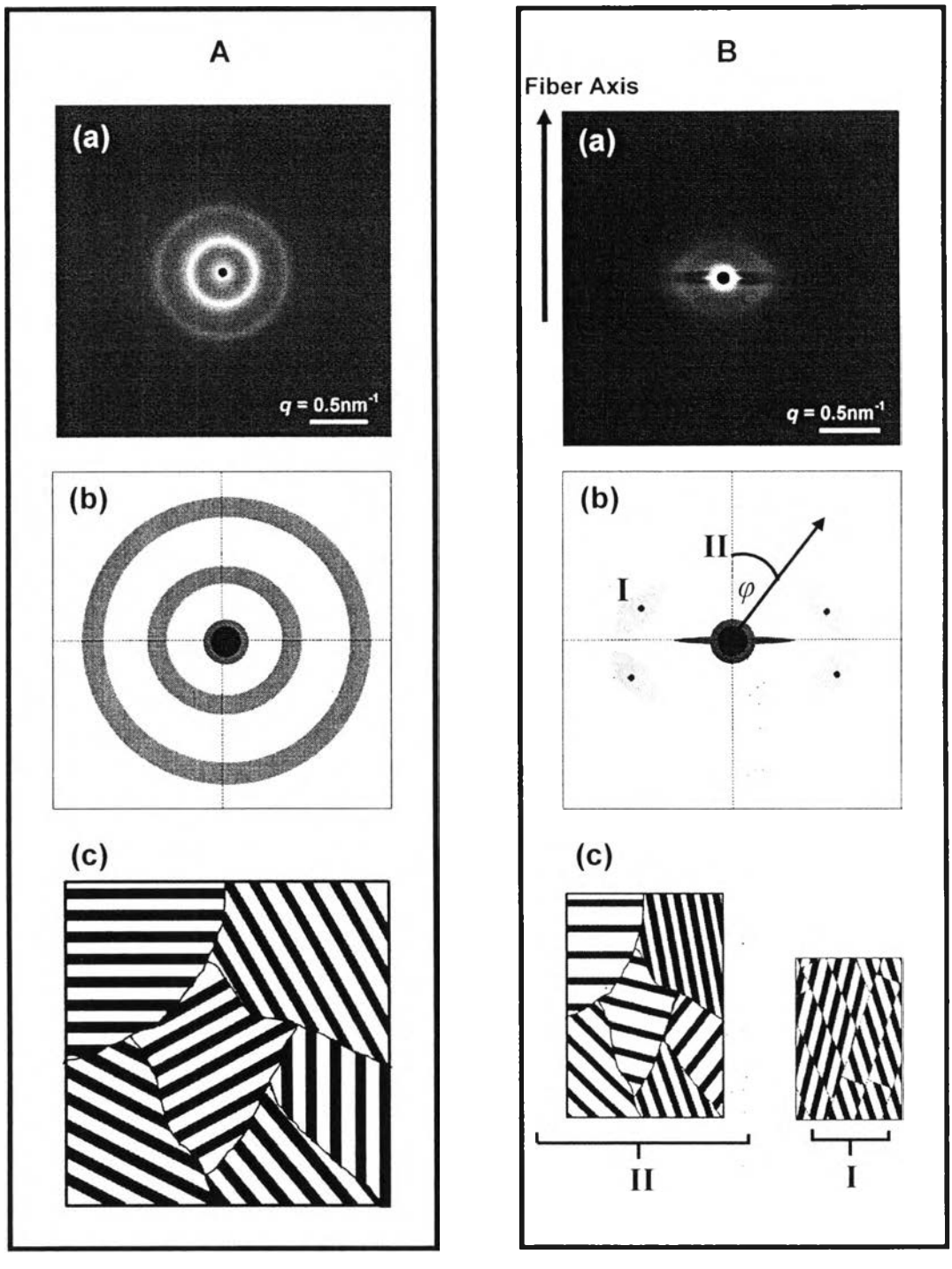

Figure 3.4 (a) 2D-SAXS patterns in a logarithmic scale for the scattering intensity (b) schematic 2D-SAXS patterns, and (c) possible schematic models to represent (a) for SEBS film (A), and SEBS electrospun fibers collected at 31.5 m/min (B).

3.4.2 Microdomain Orientation

The electrospun fibers were handled with care to avoid spoiling the microdomains and were set in the ethanol-filled chamber for 2D-SAXS measurements. There might be some differences in orientation level based on the plural fibers containing in a bundle of fibers, however, it should be pointed out here that the results obtained represented the average characters of fiber alignment regarding to those plural fibers. In other words, it is presumed that all fibers in each bundle have more or less identical internal structure. Figure 3.4B (a) shows a 2D-SAXS pattern revealing microdomains with orientation, which is dramatically different from that of the film. In other words, the result not only shows the microdomain formation as reported previously[18, 19] but also for the first time, unveils the existence of short-range ordered microdomains and the microdomain orientation of thermoplastic elastomer in the as-spun electrospinning fiber. Figure 3.4B (b) highlights two important aspects, i.e., (i) a relatively intense four-spot pattern (pattern I), and (ii) a weak elliptical peak (pattern II). The four-spot pattern suggests microdomain arrangement[22, 23] whereas elliptical pattern implies microdomain distortion[25, 26] as can be schematically drawn in Figure 3.4B (c). The four-spot pattern, so-called herringbone structure, might come from the fracture of the glassy lamellar microdomains, and/or clusters of the tiny grains oriented obliquely to the stretch direction.

To clarify the four-spot pattern, an intensity distribution along the elliptical peak as a function of the azimuthal angle, φ, was traced (Figure 3.5(a)). Here, φ is considered in clockwise starting from φ =0 at the meridional direction pointing upward (parallel to the fiber axis). The azimuthal scans for the fibers obtained show four-spot pattern where the peaks appear at about 65°, 115°, 245° and 295°. This implies important information, i.e., an existence of microdomain orientation. In fact, this type of four-spot pattern is exactly similar to those reported by Séguela and Prud'homme for the fractured lamellar microdomains of the stretched SBS triblock copolymer film resulting in microdomain orientation.[24] In other words, their results support us about the microdomain orientation in our SEBS electrospun fibers. It should also be noted that the fibers obtained from different rotational

collector speeds show a similar four-spot pattern with the same peak positions. This confirms that the microdomain orientation exists in all cases of the fibers.

Figures 3.4B (a) and (b) clearly show that the repeating period is maximal in the lamellar direction perpendicular to the fiber axis and it decreases with an increase in φ. This refers to the elliptical pattern (pattern II). Shin et al. and Mita et al. reported that the weak elliptical pattern indicated a distortion of the lamellar microdomains.[25, 26] In addition, a dark streak (Figure 3.4 B (a)) is observed in the equatorial direction which is similar to those reported by Kume et al.[27] and Moses et al.[28] Although microdomain orientation may occur in various directions, the dark streak in the direction perpendicular to the fiber axis indicates the lack of the microdomain oriented in the direction parallel to the fiber axis.

The microdomain orientation in electrospun fibers might be due to the stress field while the fibers were drawn. Therefore, we speculated that the microdomains might form in the first step when the polymer solution was solidified in the spin line. At that time an orientation, which depends on the stress field applied to the fibers, might generate. This can be seen from an elliptic SAXS pattern. As the stress was more intense, the lamellar microdomains were aligned parallel (or almost parallel) to the fiber axis, and, at a certain stress level, the microdomains were fractured resulting in the lack of parallel-lamellar microdomains. As a consequence, the fractured lamellar oriented obliquely to the fiber axis to give four-spot pattern in 2D-SAXS pattern.

It should be noted that in most cases, the plate collector is used to collect the electrospun fibers. As the fibers are randomly spread on the collector, there is no alignment. However, in our case, the fibers were carefully collected on a rotational disk collector with a controllable rotating speed. This initiates the fibers to align in the rotating direction and allowed us the morphological analysis in details, especially by using 2D-SAXS.

It comes to our question whether an increase in rotational speed relates to an increase in microdomain orientation or not. Therefore, the fibers were collected at various take-up velocities, i.e., 31.5 m/min, 310 m/min, 620 m/min and 1 240 m/min, and the fiber diameter obtained were found to be 6.3 μm, 4.6 μm, 3.3 μm and 2.5 μm, respectively. Surprisingly, the fibers collected at the lowest rotational

disk speed (31.5 m/min, Figure 3.5(a)) shows the most intense peaks as compared to the fibers collected from other high rotational speeds (Figures 3.5(b)-3.5(d)).

It is clear that although the take-up velocities of the rotational disk collector were varied, the 2D-SAXS patterns of each fiber are similar. When the elliptical patterns were considered carefully, it was found that the SEBS electrospun fibers collected at the lowest take-up velocity (31.5 m/min) shows the most significant elliptical shape. From Figures 3.5(b)-(e), the first-order scattering maxima at $\varphi = 0°$ and $\varphi = 90°$ for q_0 and q_{90}, respectively, were measured and summarized in Table 3.1. The r ($= q_{90}/q_0$) value quantifies the extent of distortion in the lamellar repeating distance. For the cast film, the r ratio is about one, indicating an isotropic lamellar. On the contrary, the r values for the electrospun fibers are in the range of 1.15-1.24 indicating anisotropic lamellae. Especially, the electrospun fibers collected at 31.5 m/min show the highest r value (1.24), confirming the most distorted lamellae. However, it should be noted that the r values of all samples are close, not that much shift from one (as small as 1.3 nm or even less than this).

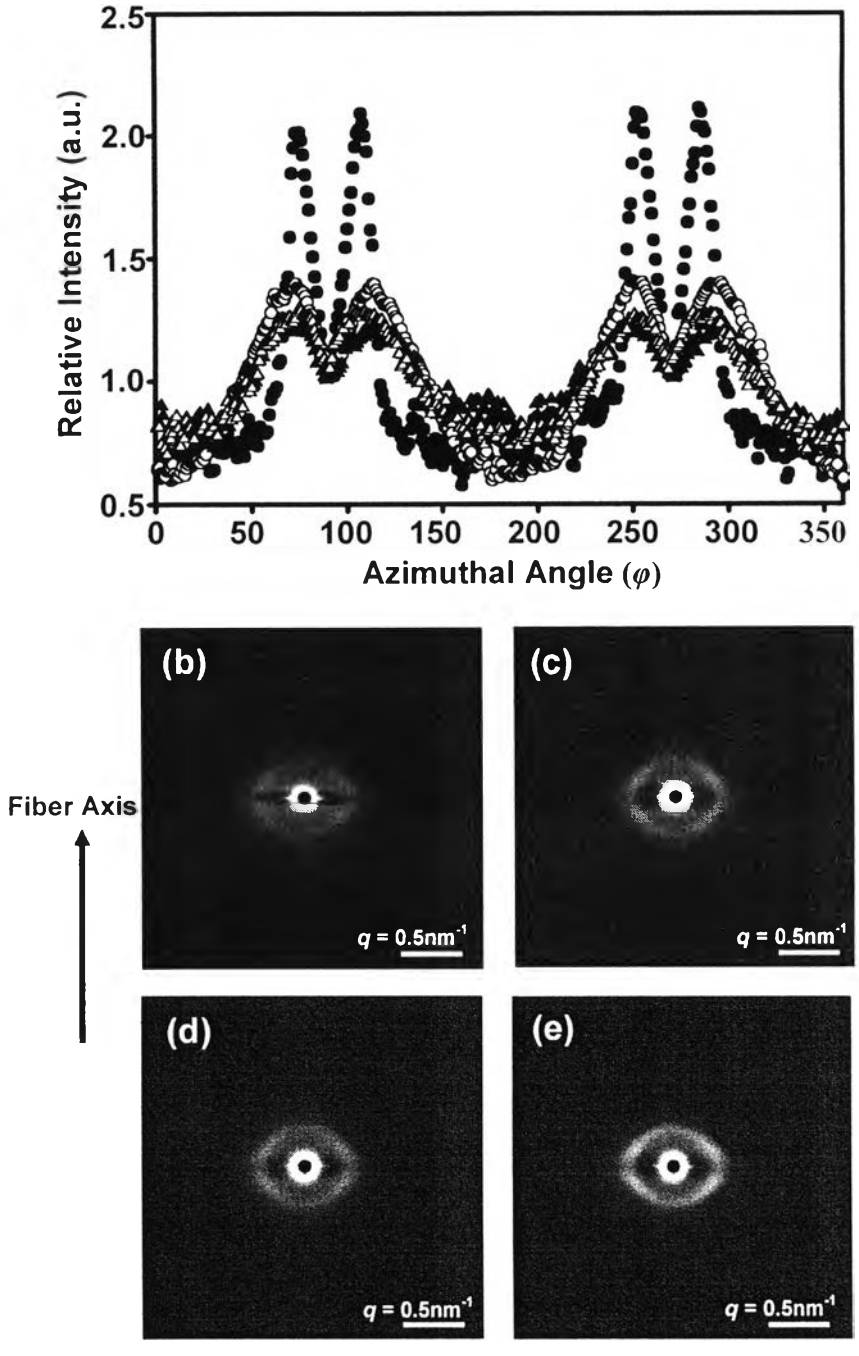

Figure 3.5 2D-SAXS patterns of the fibers collected at: (a) 31.5 m/min, (b) 310 m/min, (c) 620 m/min, (d) 1 240 m/min; and (e) intensity distribution as a function of the azimuthal angle φ along the elliptic peak (azimuthal scan) of the SEBS electrospun fibers collected at 31.5 m/min (●), 310 m/min (○),620 m/min (▲) and 1240 m/min (△).

Table 3.1 Peak positions, q_0 *and* q_{90}, and lamellar repeating period for φ = 0° and φ = 90°, respectively, obtained from 2D-SAXS patterns of SEBS electrospun collected at various take-up velocities compared with those of bulk film

Sample	Peak positions (nm^{-1})[a]		*r* ratio	Lamellar repeating period (nm)[b]	
	q_0 at azimuthal angle ϕ = 0°e	q_{90} at azimuthal angle ϕ = 90°e	(q_{90}/q_0)	Azimuthal angle ϕ = 0°e	Azimuthal angle ϕ = 90°e
Cast film	0.243	0.239	1.02	25.9	26.4
Electrospun at 31.5 m/min	0.286	0.355	1.24	21.9	17.7
Electrospun at 310.0 m/min	0.305	0.350	1.15	20.6	17.9
Electrospun at 620.0 m/min	0.298	0.349	1.17	21.1	18.0
Electrospun at 1240.0 m/min	0.290	0.341	1.17	21.6	18.4
Anneale[d] electrospun at 620.0 m/min	0.274	0.281	1.03	22.9	22.3
Annealed electrospun at 1.240.0 m/min	0.274	0.284	1.02	22.9	22.1

[a] measured at the first-order scattering maximum

[b] calculated by Bragg's equation

[c] φ azimuthal angle with respect to fiber axis for the 2D-SAXS patterns

[d] annealing at 170°C for 3 hours.

Based on the herringbone structure, five structural parameters from 2D-SAXS pattern were further evaluated.[22] Figure 3.6 shows schematic explanations for those parameters in both 2D-SAXS pattern (Figure 3.6b) and lamellar-microdomain model (Figure 3.6c). The magnitude of q vector, which can be calculated from the repeating lamellar period (d) as $d = 2\pi/q_m$, is q_m. The widths of the elliptical spots are assigned to the parameters σ and δ, as shown in Figure 3.6b. These parameters are inversely proportional to the size of a lamellar grain as shown in Figure 3.6c. The angle between the q vector and fiber axis is assigned to the parameter μ while an oblique angle of the elliptical spot with respect to the fiber axis is assigned to ϕ. For the lamellar-microdomain model, μ and ϕ are ascribed to the angle between the fiber axis and the vector normal to lamellar microdomains (n_L) and the one normal to the grain (n_G) respectively.

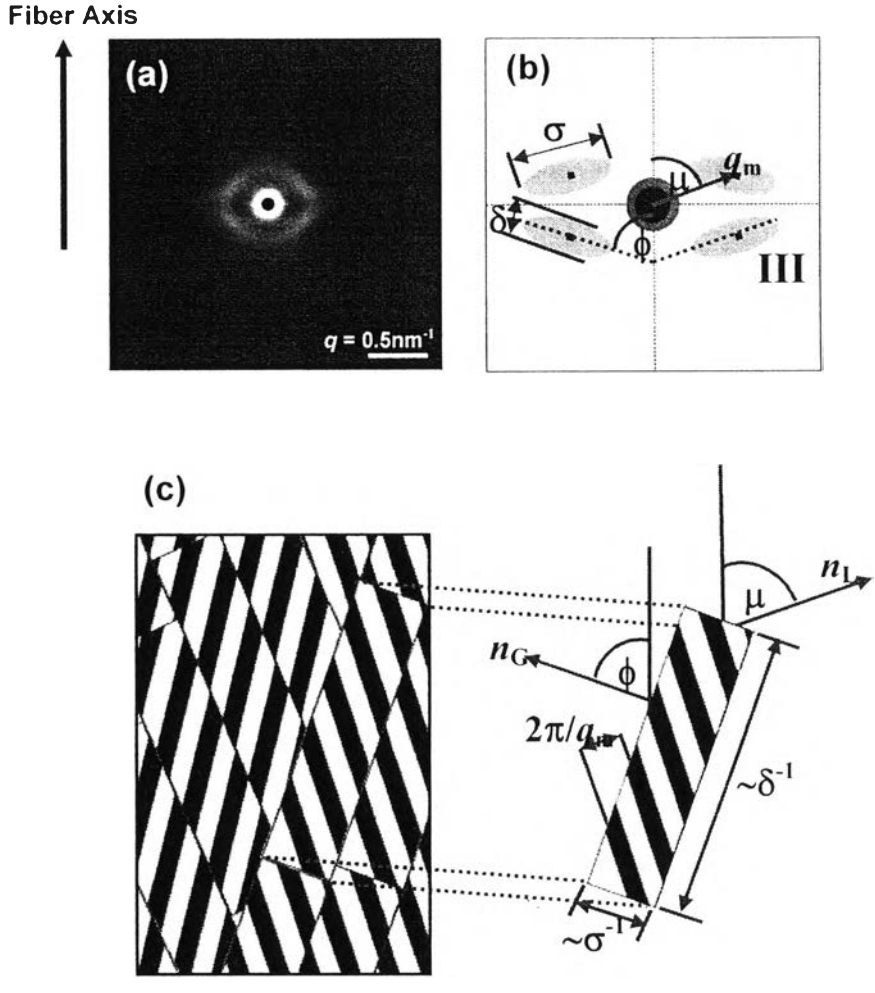

Figure 3.6 2D-SAXS patterns of the fibers collected at (a) 620 m/min, (b) schematic draw including structural parameter, and (c) possible lamellar-microdomain models including structural parameter.

As shown in Figure 3.7, the q_m value slightly decreases, or in other words, the lamellar repeat period (d) increases, as the take-up velocity increases. The stretching of lamellar microdomains can also be confirmed from the decreases of σ and δ. Figure 3.8 shows that when the take-up velocity increases, the grain size of the lamellae increases. This can be schematically illustrated in Figure 3.10. It should be noted that the decrease in q_m, and the increases in σ and δ with the take-up velocity are not that significant and at the same time the parameters μ and ϕ are maintained at

about 40° and 80°, respectively (Figure 3.9). These quantitative analyses confirm the existence of orientation in microdomain, though it is slightly. This leads to the point how we can improve orientation of SEBS electrospun fibers which will be reported in our up-coming article.

Here, we propose two possible factors to control the microdomain distortion and orientation in the as-spun electrospinning fiber upon applying shear force from rotational-disk collector. The first one is the shearing factor which promotes the microdomain stretching and orientation. When the fibers were collected at high speed, the fibers were stretched as a consequence of the shear stress at the first contact between the collector and the spinning jet. This brought in the reduction of the fiber diameters, microdomain distortion and orientation. Therefore, we could observe the stretching of the herringbone structure only when the fibers were collected from the take-up velocity less than 620 m/min as summarized in Figure 10. The second one is the solvent evaporation during spinning which causes vitrification of PS microdomains. The time for solvent evaporation of the fiber obtained via the high rotational collector speed is short as compared to the one via the low collector speed. In the case of the lowest take-up speed, 31.5 m/min, during the fibers were stretched on the rotational disk collector; the solvent evaporation might be completed. As a result, we can observe the most significant lamellar distortion from the fibers obtained from the lowest take-up speed (31.5 m/min).

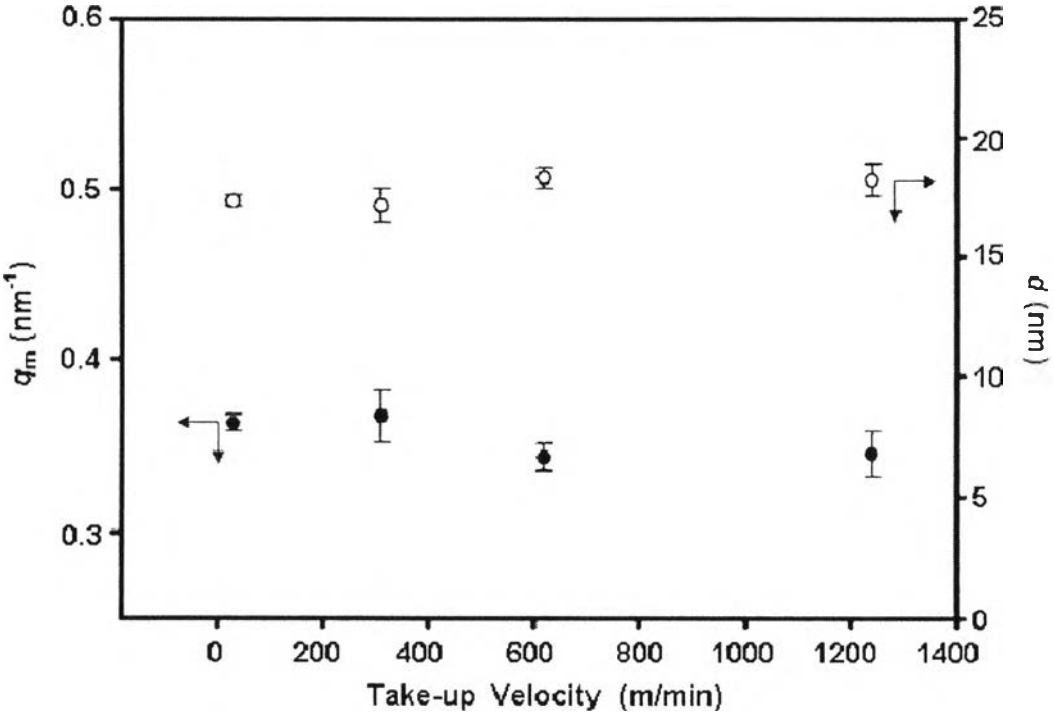

Figure 3.7 Parameters q_m (the magnitude of q vector at the peak), and d (lamellar repeating periods) of the SEBS fibers collected at various take-up velocities.

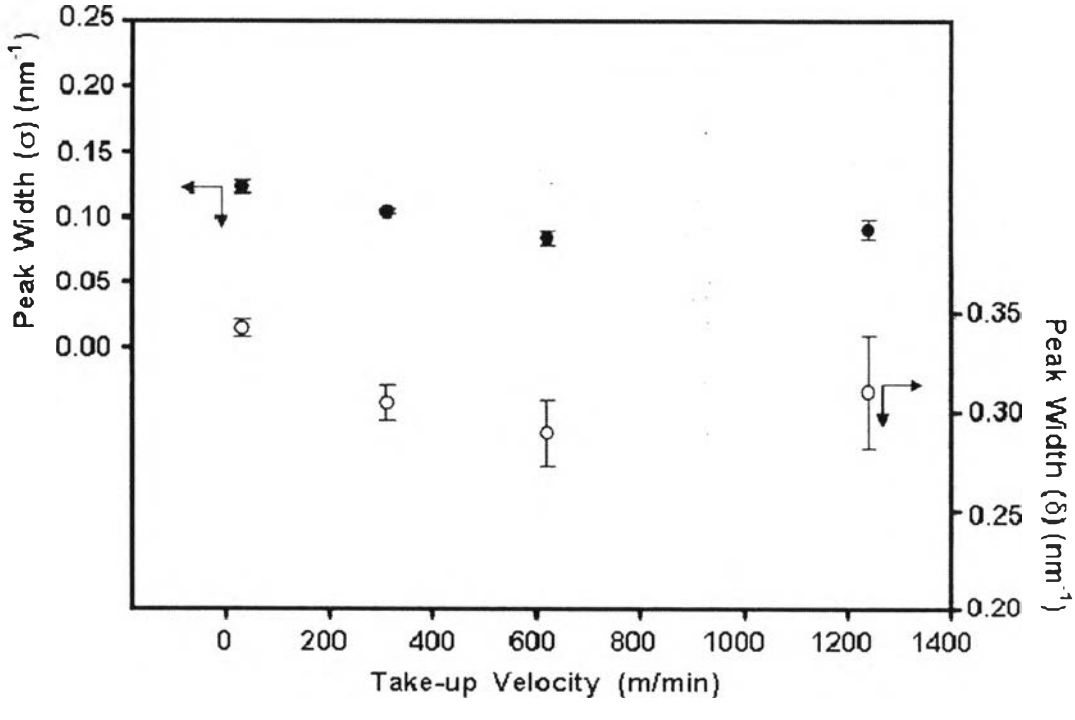

Figure 3.8 Peak width σ , and δ of the SEBS fibers collected at various take-up velocities.

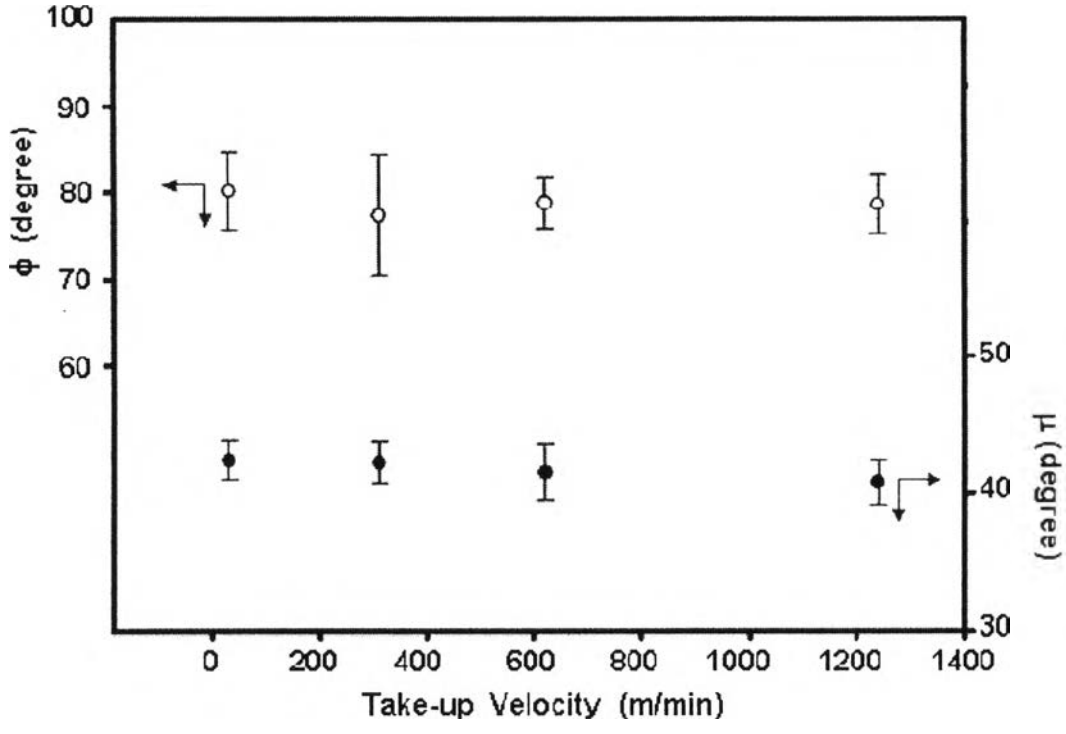

Figure 3.9 Angle μ , and ϕ of the SEBS fibers collected at various take-up velocities.

To conclude the development of the lamellar microdomains in the as-spun fibers, the lamellar-microdomain model was schematically drawn in Figure 3.10. Figure 3.10(a) shows distorted lamellar microdomains to represent elliptic pattern, whereas Figure 3.10(b) shows fragmented-lamellar microdomains, herringbone structure, to represent four-point pattern. Here, the take-up velocity induced significant differences in size of fragmented-lamellar grain. Figure 3.10(c) is a schematic to emphasize how the grain size (δ^{-1} and σ^{-1}) is increased as the take-up velocity increased.

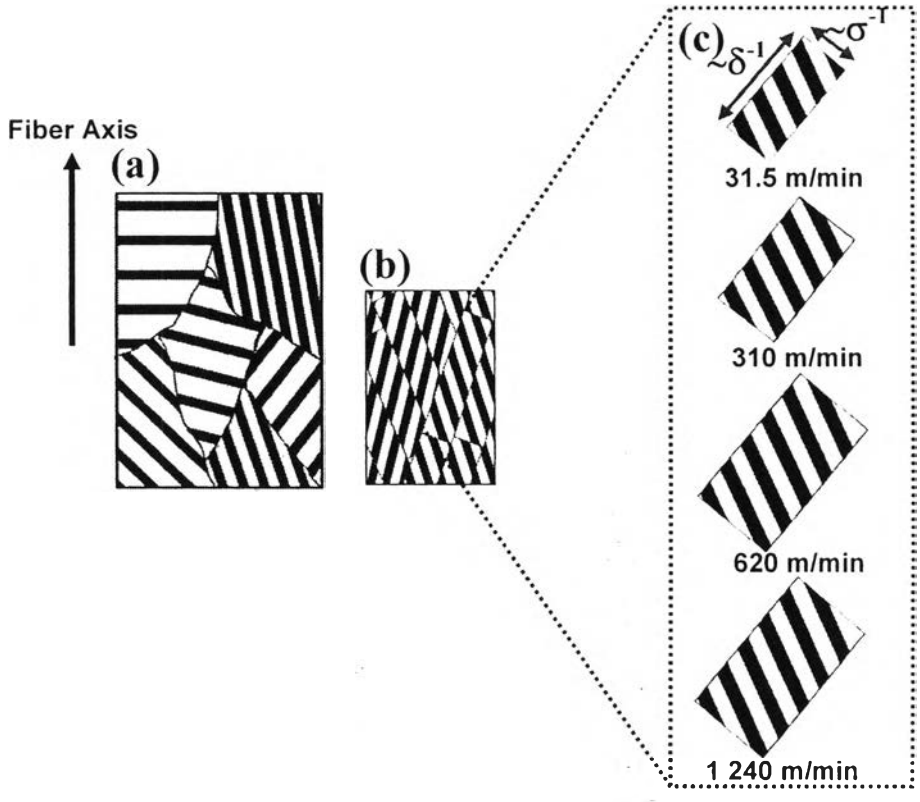

Figure 3.10 Possible models of: (a) distorted-lamellar microdomains, (b) fragmented-lamellar microdomains in the SEBS fibers at various take-up velocities, (c) schematic grain size (δ^{-1} and σ^{-1}) regarding to take-up velocities.

To examine the effect of thermal annealing, the 2D-SAXS patterns for the thermally annealed fiber samples were measured. In order to avoid the melt fracture of the fibers during thermal annealing, the fibers were coated with epoxy followed by annealing at 170 °C for 3 hours. Figure 3.11 reveals the lamellar microdomains retained after annealing. Sakurai et al. reported a microdomain orientation in crosslinked SBS film under uniaxial stretching at a temperature above its Tg (130 °C) as analyzed by SAXS pattern[16]. In our case, adhesive epoxy was used to fix the fiber dimension, so that some extent of the maintaining force against shrinkage would be anticipated. It should be noted that the electrospun fibers were annealed without any physical constraints such as clamping. Figure 3.11(a) shows the 2D SAXS pattern of the fibers obtained from the condition using the disk

collector speed at 1 240 m/min followed by thermal annealing. The annealing brings in the isotropic 2D-SAXS pattern with traces of a pair of distinct spots in the equatorial direction. This suggests an orientation of the microdomain lamellae parallel to the fiber axis which was once existed in the fiber. Thermal annealing also diminishes anisotropy in the lamellar repeating distance, irrespective of the azimuthal angle. As shown in Table 3.1, the annealed electrospun fibers show the decreases of r values from 1.17 to 1.03, which is similar to that of the film. This implies the change of anisotropic to isotropic microdomains upon the thermal annealing. In the case of the fibers collected by a take-up velocity at 620 m/min (Figure 3.11(b)), the microdomains are weakly oriented in two directions parallel and perpendicular to the fiber axis, respectively. This can be more clearly observed from the four peaks in the azimuthal profile in Figure 3.11(c).

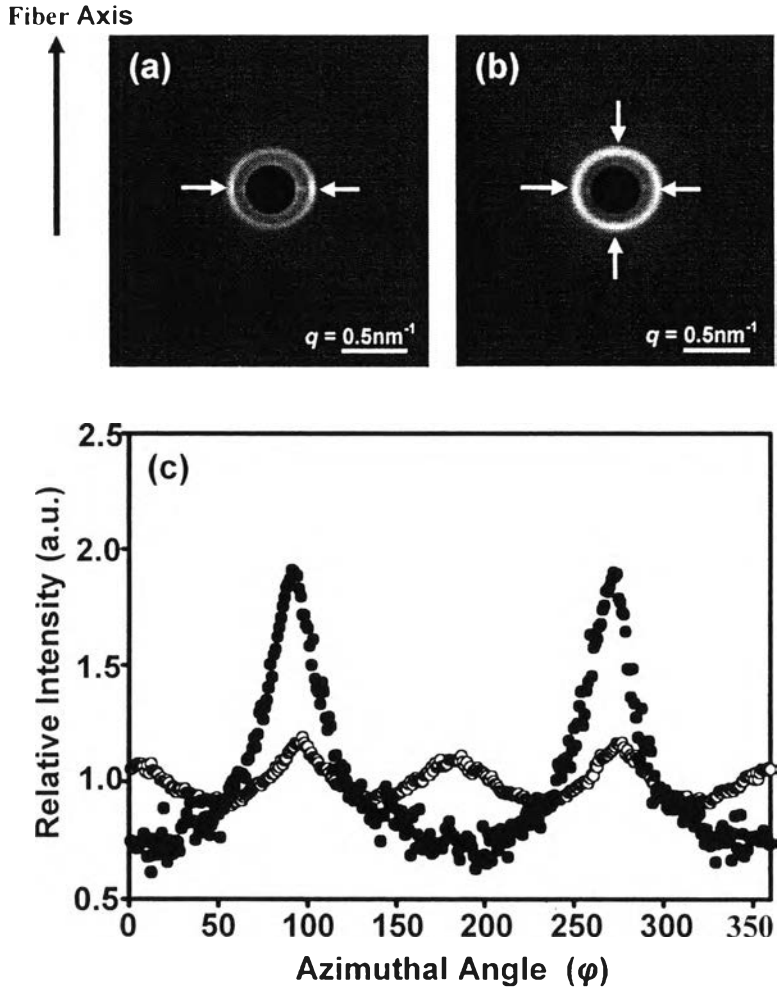

Figure 3.11 2D-SAXS patterns in a logarithmic scale of: (a) 1 240 m/min, and (b) 620 m/min and; (c) azimuthal-scan profile for annealed SEBS electrospun fibers collected at 1240 m/min (●) and 620 m/min (○).

3.5 Conclusions

Up to the present, thermoplastic elastomers are known about isotropic morphological microdomain which can be clearly seen by TEM. The present work, for the first time, demonstrates an existence of microdomain orientation through a case study of electrospun SEBS. In order to study on this, the electrospinning system was equipped with a rotational disk collector to allow the fiber alignment and control the fiber shear rate whereas the 2D SAXS sample chamber was filled with ethanol to observe microdomain without the disturbance of the streaks. The 2D-SAXS of the

electrospun SEBS fibers qualitatively showed elliptical pattern implying microdomain distortion and four-spot pattern suggesting an arrangement and orientation of fragmented microdomains. The fibers collected at the lowest rotational disk speed (31.5 m/min) showed the most significant elliptical shape in SAXS pattern as compared to the fibers collected from other higher rotational speeds. The microdomain distortions of the fibers collected from all rotational disk speed were quantitatively analyzed based on the r values of the first-order scattering maxima at φ = 0° and φ = 90°. The values of the electrospun fibers collected at 31.5 m/min showed the highest r value (1.24) and overall they were in the range of 1.15-1.24 indicating anisotropic lamellae. By simply annealing the electrospun fibers, the r values were reduced to about 1, suggesting the change of anisotropic to isotropic microdomains. We speculate that the microdomains might form as soon as the polymer solution was ejected from the needle and at that time the shearing promotes the microdomain stretching and orientation whereas the solvent evaporation causes verification. Therefore, the fibers obtained from the lowest rotational disk take up velocity were stretched in a certain time for solvent evaporation completion resulting in the most significant lamellar distortion.

As the present work shows the microdomains of electrospun fibers with diameter at micrometer scale, there might be a question whether these microdomains are existed in fibers at nanometer scale or not. The fact that SEBS in chloroform/toluene has relatively low conductivity; this obstructed us to obtain the fibers in nanometer level to answer the above question. However, as the TEM images of our fibers and of those in previous reports are similar, we speculated that the microdomains should exist in those nanofibers. In addition, as the stretch based on electrostatic force is one of the key factors to control the fibers to be nanometer size, it is natural to expect to see the ordered-microdomain orientation. We believe that a good sample preparation with 2D-SAXS analyses of nanofibers should provide us exact information about the ordered-microdomain orientation.

3.6 Acknowledgements

S. C. and W. R. would like to express their gratitude to the Royal Golden Jubilee Program (the Thailand Research Fund (PHD/0058/2550)), and the Japan Student Services Organization (JASSO). The authors acknowledge Dr. Eiko Nakazawa and Akiko Fujisawa for microtoming, and the Hitachi High-Technologies Corporation, Japan, for TEM measurement. The gratitude is also to Asahi Kasei Chemicals Corporation, Japan for SEBS. The SAXS measurements were conducted at the SPring-8 under the approved number 2009A1153.

3.7 References

1. Holden G, Kricheldorf HR, Quirk, RP. In Thermoplastic Elastomers, Edition 3rd, Hanser Verlag 2004; p 2-3.
2. Spontak RJ, Patel NP. Current Opinion in Colloid & Interface Science 2000; 5: 334-341.
3. Bhowmick, AK, Stephens HL. In Handbook of Elastomers, Edition 2nd, CRC Press 2000; p 327-330.
4. J A Brydson, Rapra Technology Limited, In Thermoplastic Elastomers: Properties and Applications, iSmithers Rapra Publishing 1995; p 3-7.
5. Schweitzer PA. In Corrosion Resistance of Elastomers, CRC Press 1990; p 69-71.
6. Wang Y, Hong X, Liu B, Ma C, Zhang C. Macromolecules 2008; 41: 5799-5808.
7. Heck B, Arends P, Ganter M, Kressler J, StÜhn B. Macromolecules 1997; 30: 4559-4566.

8. Figueiredo P, Geppert S, Brandsch R, Bar G, Thomann R, Spontak RJ, Gronski W. Macromolecules 2001; 34: 171-180.

9. Ma M, Titievsky K, Thomas EL, Rutledge GC. Nano Lett. 2009; 9(4); 1678-1683.

10. Mogi Y, Kotsuji H, Kaneko Y, Mori K, Matsushita Y, Noda I. Macromolecules 1992; 25: 5408-5411.

11. Kim J, Kim B, Jung B, Kang YS, Ha HY, Oh I, Ihn KJ. Macromol. Rapid. Commun 2002; 23: 753-756.

12. Liu Y, Li M, Bansil R, Steinhart M. Macromolecules 2007; 40: 9482-9490.

13. Sakurai S, Momii T, Taie K, Shibayama M, Nomura S. Macromolecules 1993; 26: 485-491.

14. Sakurai S, Kawada H, Hashimoto T. Macromolecules 1993; 26: 5796-5802.

15. Honeker CC, Thomas EL. Chem. Mater 1996; 8: 1702-1714.

16. Sakurai S, Aida S, Okamoto S, Ono T, Imaizumi K, Nomura S. Macromolecules 2001; 34: 3672-3678.

17. Ramakrishna S, Fujihara K, Teo WE, Teo TE, Ma Z. In An Introduction to Electrospinning and Nanofibers, World Scientific Publishing Co. Pte. Ltd. 2005.

18. Fong H, Reneker DH. J. Polym. Sci. Part B Polym. Phys. 1999; 37: 3488-3493.

19. Ma M, Krikorian V, Yu JH, Thomas EL, Rutledge GC. Nano Lett. 2006; 6(12): 2969-2972.

20. Kalra V, Kakad PA, Mendez S, Ivannikov T, Kamperman M, Joo, YL. Macromolecules 2006; 39: 5453-5457.

21. Kobori Y, Kwon YK, Okamoto M, Kotaka, T. Macromolecules 2003; 36: 1656-1664.

22. Polis DL, Winey KI. Macromolecules 1996; 29: 8180-8187.

23. Sakurai S, Aida S, Okamoto S, Sakurai K, Nomura S. Macromolecules 2003; 36: 1930-1939.

24. Séguela R, Prud'homme J. Macromolecules 1981; 14: 197-202.

25. Shin G, Sakamoto N, Saijo K, Suehiro S, Ito K, Amemiya Y, Hashimoto T. Macromolecules 2000; 33: 9002-9014.

26. Mita K, Tanaka H, Saijo K, Takenaka M, Hashimoto T. Polymer 2008; 49: 5146-5157.

27. Kume T, Hashimoto T. "String Phase in Semidilute Polystyrene Solutions under Steady Shear Flow" In Flow-induced structure in polymers, American Chemical Society. 1995; p 35-47.

28. Moses E, Kume T, Hashimoto T. Phys. Rev. Lett. 1994; 72: 2037-2040.